Supporting information

$CsPbBr_3$ Crystal Growth via Antisolvent vapor assisted Method and Their Photoelectric Properties

Maksym Pecherkin[1,*], Vasyl Mykhailovych[2,*], Matthias Gutmann[3], Gheorghe Lucian Păscuț[4], Petro Fochuk[1,*], Mariia Mykhailovych[5], Aurelian Rotaru[5], Yuriy Khalavka[1], Andriy Dmytruk[6]

1 Department of Chemistry and Food Expertise, Yuriy Fedkovych Chernivtsi National University, 2, Kotsjubynskyi St., 58012 Chernivtsi, Ukraine

2 Technology Transfer Center in Industry 4.0 and Smart Destinations & Department of Electrical Engineering and Computer Science, , Stefan cel Mare University of Suceava, 720229 Suceava, Romania

3- Harwell Science and Innovation Campus, Rutherford Appleton Laboratory, ISIS Facility, Chilton Didcot, Oxfordshire OX11 0QX, United Kingdom

4 - MANSiD Research Center and Faculty of Forestry, Stefan Cel Mare University (USV), Suceava 720229, Romania

5 - Department of Electrical Engineering and Computer Science & Research Center Mansid, “Stefan Cel Mare” University, University Street, No. 13, 720229, Suceava, Romania

6 - Institute of Physics of National Academy of Sciences of Ukraine, Kyiv, Ukraine

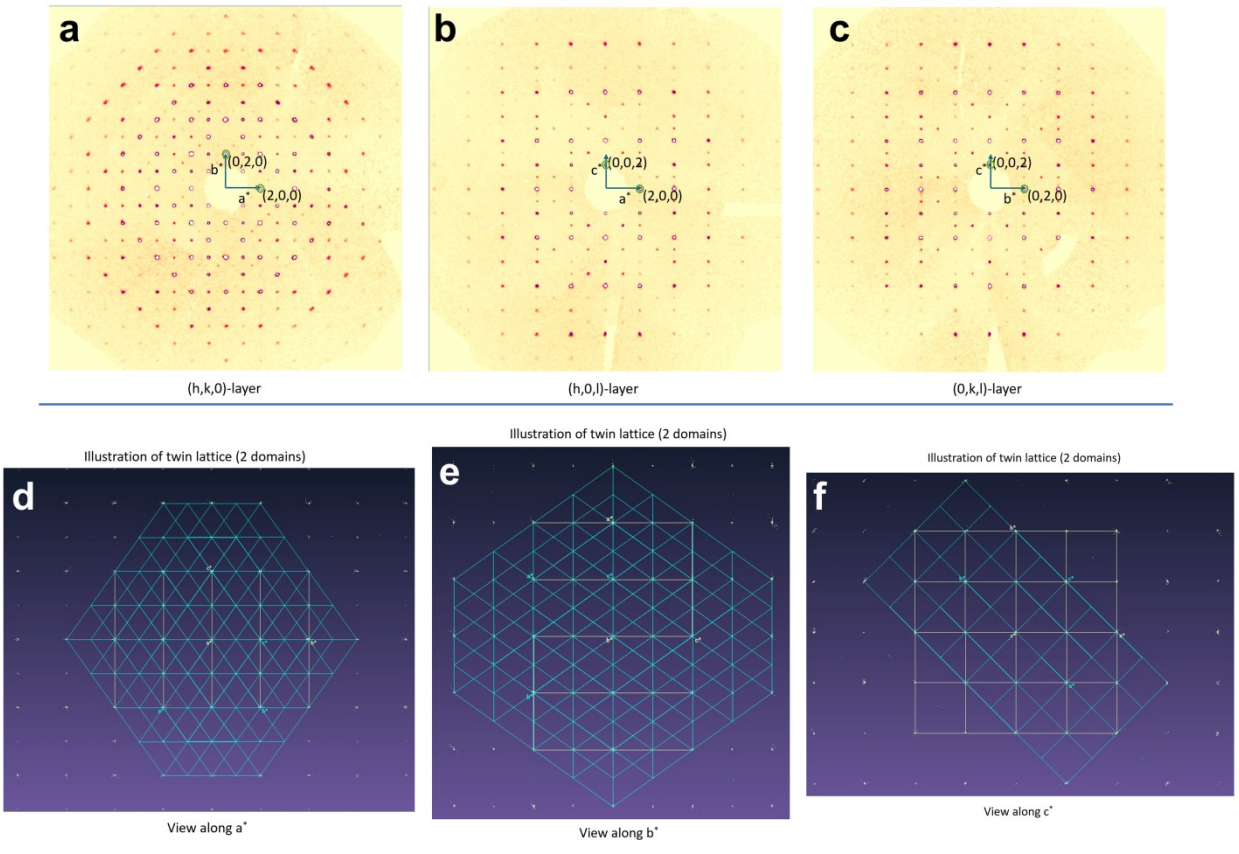

Fig. S1. Diffraction patterns for the (a) (h,k,0), (b) (h,0,l) and (c) (0,k,l). Illustration of twin lattice (2 domains) view along a (d), b (e) and c (f), where white lattice/spots correspond component 1 and blue lattice/spots correspond component 2, respectively.

Table S1: Summary of data collection and crystallographic refinement of $CsPbBr_3$.

Crystal data	
Chemical formula	$CsPbBr_3$
M_r	579.8
Crystal system, space group	Orthorhombic, Pbnm
a (Å)	8.2289(2)
b (Å)	8.2289(2)
c (Å)	11.7196(6)
V (Å^3)	793.59
Z	4
Radiation type	Mo Kα
μ (mm^{-1})	40.767
Crystal size (mm)	0.102 x 0.141 x 0.246
Data collection	
Diffractometer	Rigaku Oxford Diffraction XtaLAB Synergy, DualFlex HyPix detector
Absorption correction	Empirical
T_{min}, T_{max}	0.222, 1.0
No. of measured, independent and observed (I > 3σ(I)] reflections	20637, 3446, 1850
R_{int}	0.1419
$(\sin \theta/\lambda)_{max}$ (Å^{-1})	0.766
Refinement	
R[F^2 > 3σ(F^2)], wR[F^2 > 3σ(F^2)], R(all), wR(all), S[F^2 > 3σ(F^2)], S(all)	0.0608, 0.1393, 0.1147, 0.1528, 1.5150, 1.8885
No. of reflections	3446
No. of parameters	33
No. of restraints	0
$\Delta\rho_{max}$, $\Delta\rho_{min}$ (e Å^{-3})	3.44, -1.32
Crystal structure	
Cs x, y, z, u_{iso} (Å^2)	0.9939(3), 0.9695(2), 0.25,0.0819(10)
u_{11}, u_{22}, u_{33}, u_{12}, u_{13}, u_{23} (Å^2)	0.099(2), 0.0880(15), 0.0587(12) 0.0309(12), 0, 0
Pb x, y, z, u_{iso} (Å^2)	0.5, 0, 0, 0.0267(4)
u_{11}, u_{22}, u_{33}, u_{12}, u_{13}, u_{23} (Å^2)	0.0454(12), 0.0215(6), 0.0132(3), -0.0011(10), -0.0006(3), 0.0008(2)
Br(1) x, y, z, u_{iso} (Å^2)	0.0474(5), 0.5044(3), 0.25, 0.0851(15)
u_{11}, u_{22}, u_{33}, u_{12}, u_{13}, u_{23} (Å^2)	0.126(3), 0.119(3), 0.0110(8), 0.017(2), 0, 0
Br(2) x, y, z, u_{iso} (Å^2)	0.7934(5), 0.2061(4), 0.02435(16), 0.0665(10)
u_{11}, u_{22}, u_{33}, u_{12}, u_{13}, u_{23} (Å^2)	0.069(2), 0.0478(15), 0.0824(13), -0.0297(9), -0.0027(16), 0.0084(13)

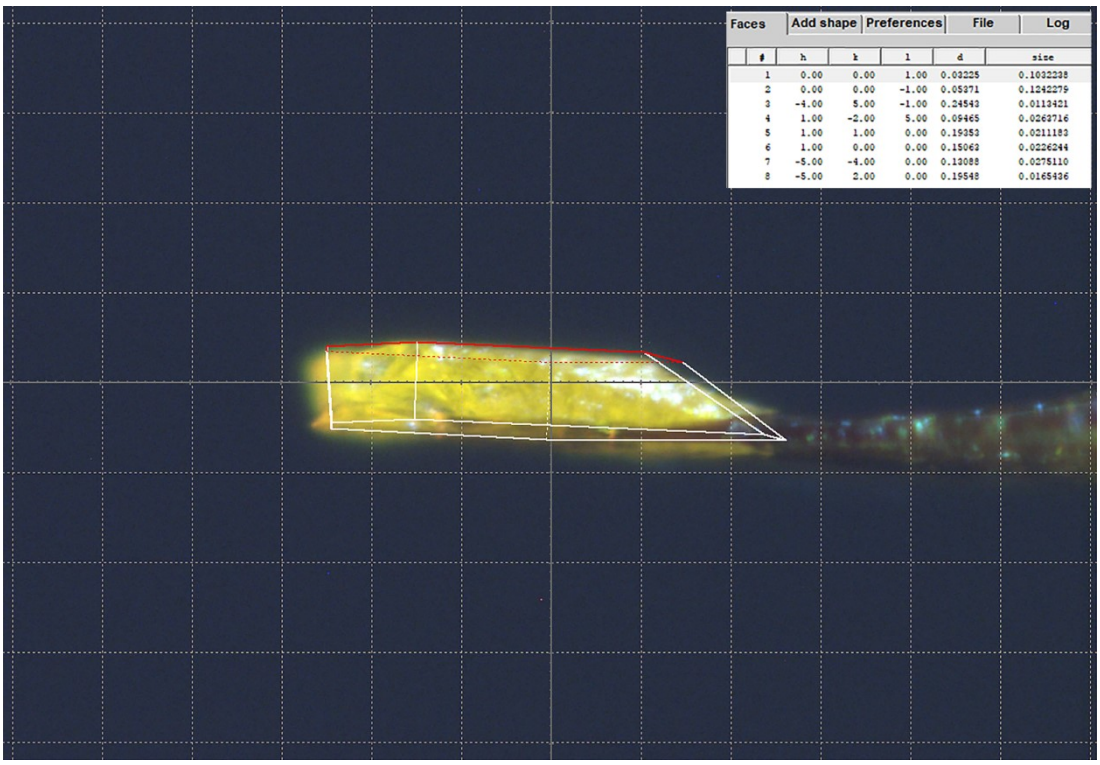

Fig. S2. Face indexing of the $CsPbBr_3$ single-crystal fragment. The indexed facets (h,k,l) and the corresponding face distances are shown in the text box.

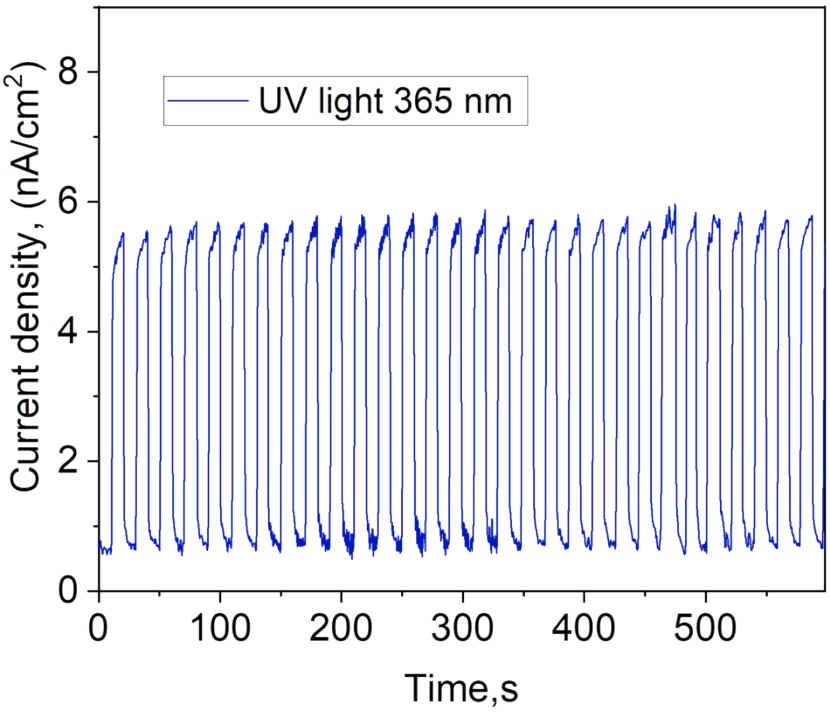

Fig. S3. Time-dependent change in photocurrent density of the $CsPbBr_3$ single crystal sample under periodic UV illumination (365 nm) during the 25 cycles.

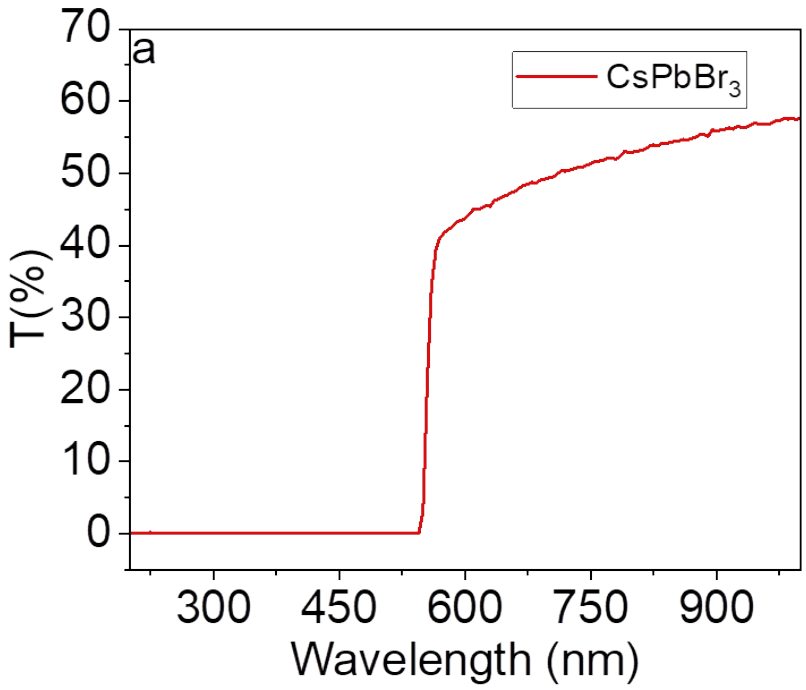

Fig. S4. V–visible transmittance spectrum of the synthesized $CsPbBr_3$ single crystal.

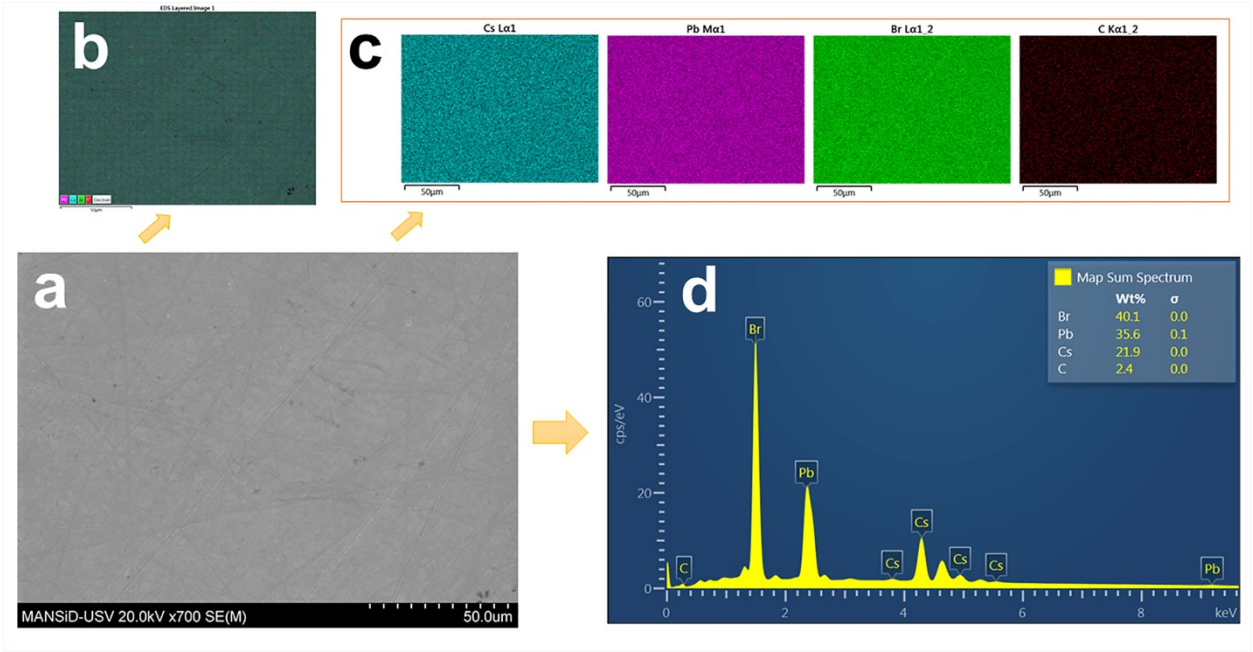

Fig. S5. Energy-dispersive X-ray (EDX) spectrum of the $CsPbBr_3$ single crystal.

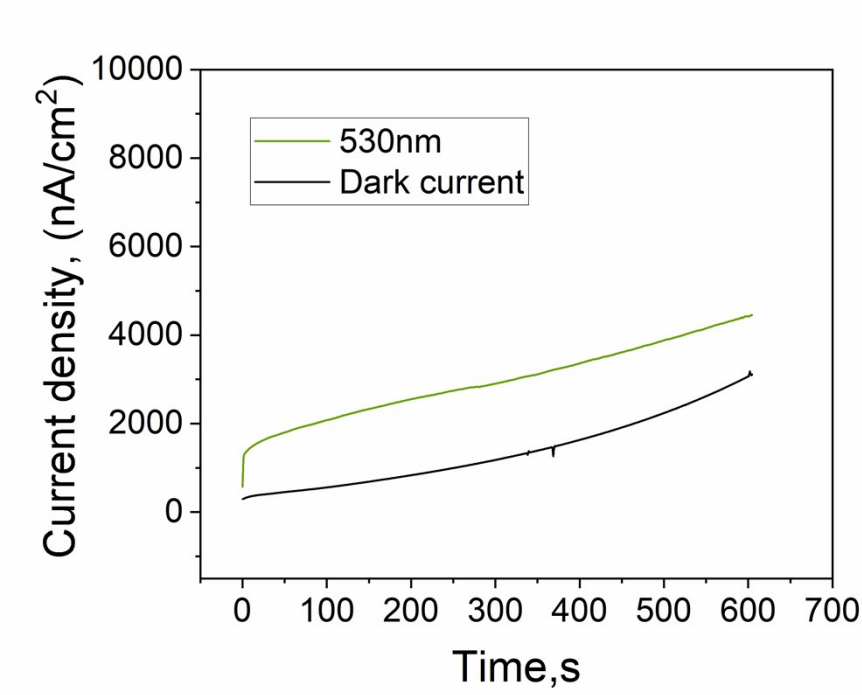

Fig. S6. I–t characteristics of the $CsPbBr_3$ single crystal recorded in the dark and under 530 nm illumination at an applied bias of +5V.

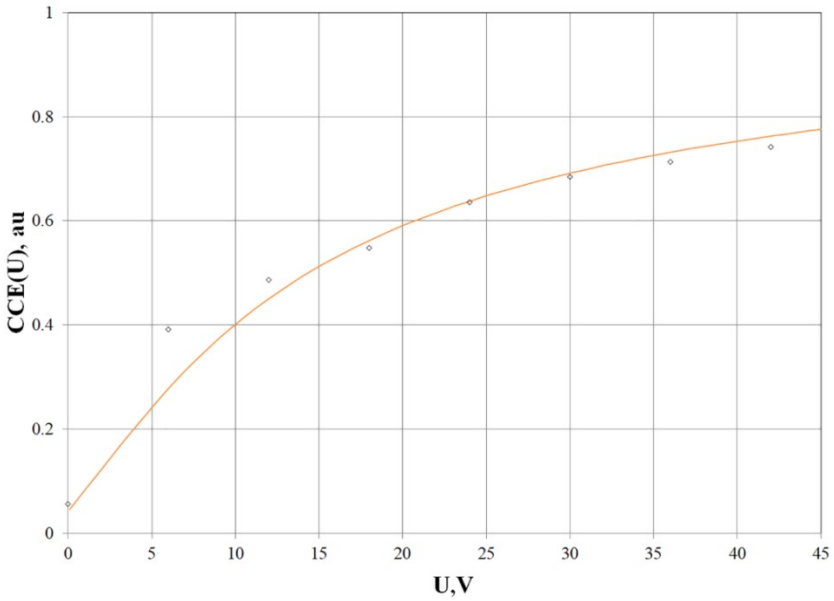

Fig. S7. Bias-dependent charge collection efficiency (CCE) of the $CsPbBr_3$ single-crystal detector. Symbols represent the experimental data, while the solid line corresponds to the fit using the Hecht equation.

Hecht measurement geometry

For the μτ evaluation, planar Au electrodes were deposited directly on the crystal surface to form a well-defined metal–semiconductor–metal (MSM) geometry suitable for Hecht-based charge collection analysis. The gold contacts had a thickness of 20 nm and a diameter of 1.5 mm, ensuring a reproducible active area and stable electrical boundary conditions during the CCE–V measurements.

Table S2. Comparison of key performance metrics for $CsPbBr_3$

Perovskite lead-based detector	Responsivity (A W^{-1})	EQE (%)	Detectivity (Jones)	Reference
$CsPbBr_3$	6.24×10^{-2}	1.5	1.29×10^{10}	This study
$CsPbBr_3$	28×10^{-3}	6	1.7×10^{11}	Saidaminov et al. [1]
$CsPbBr_3$	35×10^{-3}	8.5	1.1×10^{11}	Cheng et al. [2]
$CsPbBr_3$/ CuI	from 0.1×10^{-3} to 1.4×10^{-3}	-	6.2×10^{10}	Zhang et al. [3]
$CsPbBr_3$	2.8×10^{-2}	7	1.0×10^{11}	Ding et al.[4]

[1] M.I. Saidaminov, M.A. Haque, J. Almutlaq, S. Sarmah, X.H. Miao, R. Begum, A.A. Zhumekenov, I. Dursun, N. Cho, B. Murali, Inorganic lead halide perovskite single crystals: phase-selective low-temperature growth, carrier transport properties, and self-powered photodetection, Advanced Optical Materials, 5 (2017) 1600704.

[2] P. Cheng, Z. Liu, R. Kang, J. Zhou, X. Wang, J. Zhao, Z. Zuo, Growth and High-Performance Photodetectors of CsPbBr3 Single Crystals, ACS Omega, 8 (2023) 26351-26358.

[3] Y. Zhang, S.Y. Li, W. Yang, M.K. Joshi, X.S. Fang, Millimeter-Sized Single-Crystal CsPbrB3/CuI Heterojunction for High Performance Self-Powered Photodetector, Journal of Physical Chemistry Letters, 10 (2019) 2400-2407.

[4] J. Ding, S. Du, Z. Zuo, Y. Zhao, H. Cui, X. Zhan, High detectivity and rapid response in perovskite CsPbBr3 single-crystal photodetector, The Journal of Physical Chemistry C, 121 (2017) 4917-4923.